

Time-gated Einstein-Podolsky-Rosen correlation

Nobuyuki Takei,^{1,2,*} Noriyuki Lee,^{1,2} Daiki Moriyama,¹ J. S. Neergaard-Nielsen,^{1,3} and Akira Furusawa^{1,2}

¹*Department of Applied Physics, School of Engineering, The University of Tokyo, 7-3-1 Hongo, Bunkyo-ku, Tokyo 113-8656, Japan*

²*CREST, Japan Science and Technology Agency, 1-9-9 Yaesu, Chuo-ku, Tokyo 103-0028, Japan*

³*Niels Bohr Institute, University of Copenhagen, Copenhagen, DK 2100, Denmark*

(Received 14 July 2006; revised manuscript received 17 November 2006; published 15 December 2006)

We experimentally demonstrate the creation and characterization of Einstein-Podolsky-Rosen (EPR) correlation between optical beams in a time-gated fashion. The correlated beams are created with two independent continuous-wave optical parametric oscillators and a half beam splitter. We define the temporal modes using a square temporal filter with duration T and make time-resolved measurements on the generated state. We observe correlations between the relevant conjugate variables in the temporal mode which correspond to EPR correlation. Our scheme is extendable to continuous-variable quantum teleportation of a non-Gaussian state defined in the time domain such as a superposition of coherent states.

DOI: [10.1103/PhysRevA.74.060101](https://doi.org/10.1103/PhysRevA.74.060101)

PACS number(s): 03.65.Ud, 03.67.Mn, 42.50.Dv, 42.50.Xa

Quantum entanglement is one of the most fundamental properties of quantum mechanics and also the essential ingredient in quantum-information processing [1,2]. The non-classical correlation was first argued by Einstein, Podolsky, and Rosen (EPR) relating to canonically conjugate continuous variables (CVs) [3]. This originally devised EPR correlation has been experimentally realized by employing a two-mode squeezed state [4,5], where the relevant variables are quadrature-phase amplitudes of optical fields. Since this significant milestone, there have been further experimental observations of EPR correlations [6–12] and theoretical characterizations [13,14]. Moreover, the EPR correlation, or the two-mode squeezed state, has been used as a resource in implementation of quantum protocols. Thanks to well-established tools of manipulating the EPR correlation, CV quantum-information processing (QIP) has been rapidly developing in recent years [2] and has been successful in implementing quantum protocols such as quantum teleportation [15,16].

Quantum teleportation is one of the fundamental quantum protocols that exploit the EPR correlation or quantum entanglement [15,17]. By using an optical field, it has been experimentally realized for Gaussian input states; a coherent state [16,18–20], a squeezed state [21], and an EPR state, i.e., entanglement swapping [20,22]. These successes are based on well-developed techniques of optical Gaussian operations consisting of beam splitters, phase shifting, squeezing, phase-space displacement, and homodyne detection. In addition to teleportation, CV quantum protocols have so far been performed only with Gaussian states and operations. However, non-Gaussian states or non-Gaussian operations are further required to extract the versatile potential of CV QIP [23]. Thus quantum teleportation of a non-Gaussian state will become the next important challenge toward universal CV QIP.

For the generation of a non-Gaussian state in an optical system, there is considerable interest in the techniques where photon counting is performed for a tapped-off beam from a

Gaussian-state light beam. When counting a photon, the tapped Gaussian state is converted to a non-Gaussian state, a technique called “photon subtraction.” Recently there are some reports which show the generation of non-Gaussian states, close to a quantum superposition of coherent states $|\psi\rangle \propto |\alpha\rangle - |-\alpha\rangle$, with this technique [24,25]. Another method using photon counting, called photon addition, serves a similar role [26]. Since the photon-counting event is defined in the time domain, conventional CV teleportation schemes with a sideband of an optical carrier [16] cannot be used for the teleportation of such states. Therefore, in order to realize CV teleportation of such non-Gaussian states, one needs to generate EPR correlation in the time domain, or in a time-gated way.

In this Rapid Communication we demonstrate the experimental generation and characterization of a two-mode squeezed vacuum state in a time-gated way, a step toward CV quantum teleportation of non-Gaussian states such as a superposition of coherent states. The main feature of our EPR resource is that we use two squeezed vacuum states of continuous-wave (cw) light beams from two independent subthreshold optical parametric oscillators (OPOs) to obtain well-defined frequency and spatial modes, and also that we utilize almost the whole frequency bandwidth of the OPO cavities to define a quantum state in a temporal mode. The use of the broad bandwidth allows us to make time-resolved measurements like photon counting as described below. The experiment presented here is quite different from the previous works in the frequency domain [5–11] which dealt only with frequency sidebands a few megahertz apart from the carrier frequency, and therefore are not compatible with photon counting. Our scheme would have advantages even over the time-domain pulsed scheme [12] with respect to spatial modes. The well-defined frequency and spatial modes are important for efficient scaling of a quantum circuit via interference of several beams.

Moreover, our scheme is compatible with CV entanglement distillation with the photon subtraction operation [27]. Combining the entanglement distillation and teleportation would result in the improvement of teleportation fidelity [28]. Our entangled state could also be applicable to loophole-free tests of Bell’s inequalities [29,30].

*Electronic address: takei@alice.t.u-tokyo.ac.jp

For an ideal two-mode squeezed vacuum state with infinite squeezing, the EPR correlations can be described by the Wigner function of the two modes A and B :

$$W_{\text{EPR}}(x_A, p_A; x_B, p_B) = c \delta(x_A - x_B) \delta(p_A + p_B), \quad (1)$$

where x, p are the quadrature amplitudes corresponding to the conjugate quadrature operators \hat{x}, \hat{p} which obey the commutation relation $[\hat{x}, \hat{p}] = i/2$ ($\hbar = 1/2$) in analogy with the position and momentum operators. This Wigner function expresses that the quadrature amplitudes of the two modes are perfectly correlated ($x_A = x_B$) and anticorrelated ($p_A = -p_B$), respectively. In a real experiment where only finite squeezing is available, the state is no longer the ideal EPR state and shows finite variances in $\langle [\Delta(\hat{x}_A - \hat{x}_B)]^2 \rangle$ and $\langle [\Delta(\hat{p}_A + \hat{p}_B)]^2 \rangle$.

The two-mode squeezed vacuum generated by subthreshold OPOs has EPR correlations within the variance spectra $S_x(\Omega), S_p(\Omega)$ as usually measured in frequency-domain experiments. Here, Ω is a sideband frequency around the fundamental wavelength. When measuring cw beams in time-gated detection we need to specify a certain temporal mode within which the entangled quantum state is defined. Because of the broadband correlations of the cw beams, there is a large amount of freedom in choosing a mode that will suit an intended application and will show significant correlation below the vacuum level. For instance, in a teleportation experiment the temporal mode could be chosen to match that of the input state.

A simple choice of temporal mode is a square filter of duration T . Defining the filtered quadrature operators

$$\hat{x}^f = \frac{1}{\sqrt{T}} \int_0^T \hat{x}(t) dt, \quad (2)$$

and similarly for \hat{p}^f , these operators obey the same commutation relation $[\hat{x}^f, \hat{p}^f] = i/2$. The EPR variances within this temporal mode will be given by [31]

$$\langle [\Delta(\hat{x}_A^f - \hat{x}_B^f)]^2 \rangle = \frac{T}{2\pi} \int_{-\infty}^{+\infty} S_x(\Omega) \frac{\sin^2(\Omega T/2)}{(\Omega T/2)^2} d\Omega, \quad (3)$$

$$\langle [\Delta(\hat{p}_A^f + \hat{p}_B^f)]^2 \rangle = \frac{T}{2\pi} \int_{-\infty}^{+\infty} S_p(\Omega) \frac{\sin^2(\Omega T/2)}{(\Omega T/2)^2} d\Omega. \quad (4)$$

The variances are thus filtered by a sinc function, and by adjusting the integration time T the frequency range that contributes to the integrated correlation can be selected. The square temporal filter is simple, but not necessarily the most appropriate for an application of time-domain entanglement. Theoretical investigations concerning the shape of the filter combined with photon-counting experiments have been done in Refs. [31,32].

A schematic diagram of our experiment is illustrated in Fig. 1. This is almost the same as the entanglement preparation part in our experiment on quantum teleportation [20]. The primary source of the experiment is a cw Ti:sapphire laser at 860 nm, most of whose output is frequency doubled in an external cavity. The output beam at 430 nm is divided into two beams to pump two OPOs.

A two-mode squeezed vacuum is produced by combining

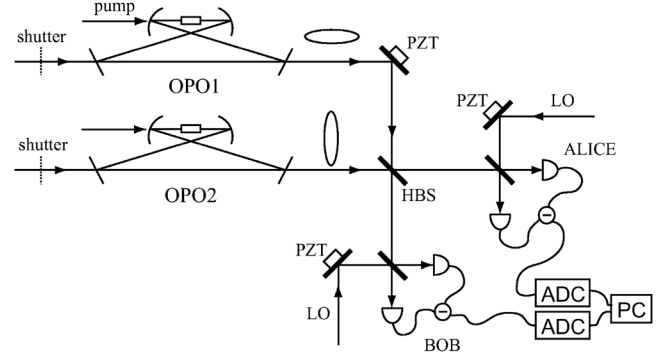


FIG. 1. Schematic setup of the experiment. OPOs, subthreshold optical parametric oscillators; HBS, half beam splitter; PZTs, piezoelectric transducers; LOs, local oscillators; ADCs, analog-to-digital converters.

two squeezed vacua at a half beam splitter (HBS). Each squeezed vacuum is generated from a subthreshold OPO with a 10-mm-long KNbO₃ crystal. The crystal is temperature tuned for type-I noncritical phase matching. Each OPO cavity is a bow-tie-type ring cavity consisting of two spherical mirrors (radius of curvature 50 mm) and two flat mirrors. The round-trip length is about 500 mm and the waist size in the crystal is 20 μm . The output coupler has transmissivity of 12.7%, while the other mirrors are highly reflective coated at 860 nm. They have a high transmission for 430 nm so that the pump beam passes the crystal only once. The pump power is about 70 mW for each OPO. The total intracavity losses are around 2%, giving a cavity bandwidth of 7 MHz half width at half maximum. The resonant frequency of the OPO is locked via the FM sideband locking method [33], by introducing a lock beam which is propagating against the squeezed vacuum beam to avoid interference between the two beams. However, a small fraction of the lock beam reflecting from surfaces of the crystal circulates backward and contaminates the squeezed state. This problem is resolved by changing the transverse mode and the frequency of the lock beam, as described in detail in Ref. [34].

The output beams from the HBS are sent to Alice and Bob, and then measured using homodyne detectors with a bandwidth of 8.4 MHz. We lock relative phases between EPR beams and local oscillators in the detection, i.e., x or p quadrature, in the following way. First, weak coherent beams which pass through the same paths as squeezed states are injected into the OPOs from one of the flat mirrors and used for the conventional dither and lock method. The relative phases between the weak coherent beams and the squeezed vacua and between the weak coherent beams at the half beam splitter are actively controlled by applying feedback voltages to piezoelectric transducers. The quadratures to be detected in the homodyne detectors are also determined by locking the phases between the LOs and the injected coherent beams. However, these weak beams and the modulation on them contaminate EPR correlation in some frequency ranges. Therefore we need to remove such beams and lock the phases without the beams. To do so, we introduce an electronic circuit that holds the feedback voltage and keeps the phase relation for a while. Within 2 ms, the beams are

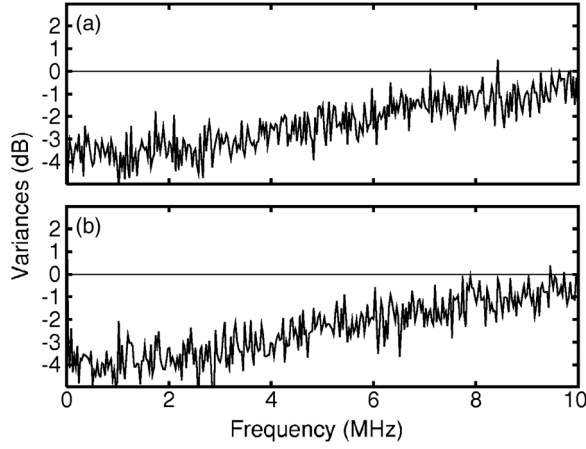


FIG. 2. Calculated Fourier analysis of the 50M-sampled raw data without average. (a) $S_x(\Omega)$ for $\langle [\Delta(\hat{x}_A^f - \hat{x}_B^f)]^2 \rangle$. (b) $S_p(\Omega)$ for $\langle [\Delta(\hat{p}_A^f + \hat{p}_B^f)]^2 \rangle$. Each trace is normalized to the corresponding vacuum level.

blocked with mechanical shutters before the OPOs, and the EPR beams are measured with homodyne detectors. Each output from the detectors is sampled with an analog-to-digital converter at a rate of 50×10^6 samples per second and then filtered on a PC to yield a number of measured quadrature values.

Before observing the EPR correlation in time-gated measurements, we estimate what range of the frequency bandwidth can be used to yield a time-resolved quadrature value from the OPOs. Figure 2 shows the frequency spectra $S_x(\Omega)$ and $S_p(\Omega)$ for the measured EPR beams calculated by performing Fourier transformation digitally on the 50×10^6 sampled raw data points. The EPR correlation is observed over the full bandwidth of the OPOs. In particular it is observed for low frequencies down to 5 kHz (a high-pass filter with a cutoff of 5 kHz is used to eliminate noise at frequencies close to dc). Correlation at low frequencies is essential for the photon subtraction experiment for non-Gaussian operation or entanglement distillation [35]. From the results, we can define a quantum state within a time interval of the inverse of the cavity bandwidth 7 MHz. But the EPR correlations degrade at higher frequencies, so we use the temporal filter (2) with integration time $T=0.2 \mu\text{s}$, yielding 10 000 points in each measurement. It follows from the frequency filters of sinc functions in Eqs. (3) and (4) that we select mainly a frequency range below 5 MHz.

First we compare explicitly the time-resolved quadrature values measured by Alice and Bob in every $0.2 \mu\text{s}$, rather than the variances of $\langle [\Delta(\hat{x}_A^f - \hat{x}_B^f)]^2 \rangle$ and $\langle [\Delta(\hat{p}_A^f + \hat{p}_B^f)]^2 \rangle$ used in the previous works [5–8]. This is also different from the pulsed scheme [12] where EPR beams were recombined at a beam splitter and returned to two squeezed vacua, one of which was then measured in homodyne detection. Figure 3 shows a typical example of the measured quadrature values within time interval $T=0.2 \mu\text{s}$, where only 50 points are picked up. As mentioned above, the measured values behave in such a way that x and p quadratures are correlated ($x_A^f \approx x_B^f$) and anticorrelated ($p_A^f \approx -p_B^f$), respectively. This manifests the originally devised correlations discussed by EPR.

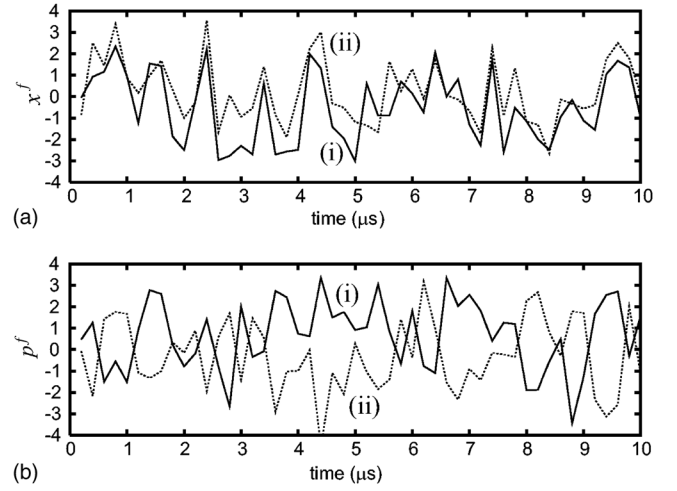


FIG. 3. Typical measured correlations. Only 50 points are picked up. (a) and (b) are measured quadrature values within the time interval $T=0.2 \mu\text{s}$ for x and p quadratures, respectively. In each figure, trace (i) is for Alice, while (ii) is for Bob.

We then estimate the degree of EPR correlation using the correlation diagrams with 10 000 points as shown in Fig. 4. These results show clear correlations in the relevant quadratures. By repeating the same measurement ten times, we obtained the correlations of $\langle [\Delta(\hat{x}_A^f - \hat{x}_B^f)]^2 \rangle = -3.30 \pm 0.28$ dB and $\langle [\Delta(\hat{p}_A^f + \hat{p}_B^f)]^2 \rangle = -3.74 \pm 0.32$ dB compared to the corresponding vacuum variances. Accordingly the sufficient criterion [13,14] for quantum entanglement holds: $\langle [\Delta(\hat{x}_A^f - \hat{x}_B^f)]^2 \rangle + \langle [\Delta(\hat{p}_A^f + \hat{p}_B^f)]^2 \rangle = 0.45 \pm 0.02 < 1$. Therefore our generated state is entangled in the temporal mode defined within $T=0.2 \mu\text{s}$. Note that we can decrease the integration time T for fast data acquisition and QIP, while the EPR correlation will degrade due to the contribution of higher-frequency ranges. One would be able to obtain correlation over a broader band by use of small-size OPOs with shorter round-trip length or waveguide crystals, e.g., periodically poled lithium niobate waveguides [36].

In summary we have experimentally demonstrated generation and characterization of a two-mode squeezed vacuum state in a time-gated fashion. We have observed the nonclassical correlation between the temporally measured quadrature values. Our setup is almost the same as an entanglement preparation part of our quantum teleportation setup [20].

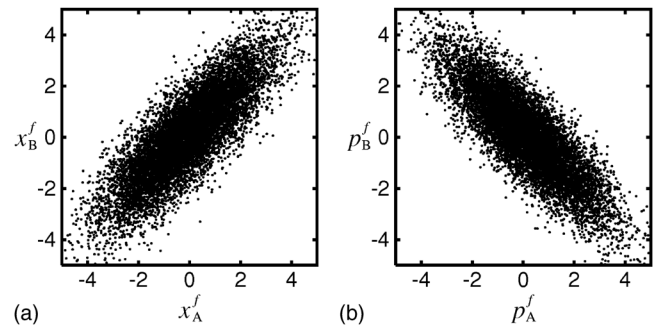


FIG. 4. Measured correlation diagrams of 10 000 measured values for (a) x and (b) p quadratures.

With slight modification of classical channels, we will be able to perform the broadband teleportation whereby it is possible to transfer quantum states defined in the time domain like a superposition of coherent states, a single-photon state, and other non-Gaussian states. Moreover our scheme is compatible with CV entanglement distillation with photon subtraction [27]. Our system has well-defined frequency,

spatial, and temporal modes. Therefore we could efficiently scale up quantum circuits by interfering several beams with the goal of universal CV QIP.

This work was partly supported by the MEXT and the MPHPT of Japan, and the Research Foundation for Opto-Science and Technology.

-
- [1] M. A. Nielsen and I. L. Chuang, *Quantum Computation and Quantum Information* (Cambridge University Press, Cambridge, U.K., 2000).
- [2] S. L. Braunstein and P. van Loock, *Rev. Mod. Phys.* **77**, 513 (2005).
- [3] A. Einstein, B. Podolsky, and N. Rosen, *Phys. Rev.* **47**, 777 (1935).
- [4] M. D. Reid, *Phys. Rev. A* **40**, 913 (1989).
- [5] Z. Y. Ou, S. F. Pereira, H. J. Kimble, and K. C. Peng, *Phys. Rev. Lett.* **68**, 3663 (1992).
- [6] Ch. Silberhorn *et al.*, *Phys. Rev. Lett.* **86**, 4267 (2001).
- [7] C. Schori, J. L. Sørensen, and E. S. Polzik, *Phys. Rev. A* **66**, 033802 (2002).
- [8] W. P. Bowen, R. Schnabel, P. K. Lam, and T. C. Ralph, *Phys. Rev. Lett.* **90**, 043601 (2003).
- [9] A. S. Villar, L. S. Cruz, K. N. Cassemiro, M. Martinelli, and P. Nussenzveig, *Phys. Rev. Lett.* **95**, 243603 (2005).
- [10] X. Su *et al.*, *Opt. Lett.* **31**, 1133 (2006).
- [11] J. Jing, S. Feng, R. Bloomer, and O. Pfister, *Phys. Rev. A* **74**, 041804(R) (2006).
- [12] J. Wenger, A. Ourjoumtsev, R. Tualle-Brouri, and P. Grangier, *Eur. Phys. J. D* **32**, 391 (2005).
- [13] L.-M. Duan, G. Giedke, J. I. Cirac, and P. Zoller, *Phys. Rev. Lett.* **84**, 2722 (2000).
- [14] R. Simon, *Phys. Rev. Lett.* **84**, 2726 (2000).
- [15] S. L. Braunstein and H. J. Kimble, *Phys. Rev. Lett.* **80**, 869 (1998).
- [16] A. Furusawa *et al.*, *Science* **282**, 706 (1998).
- [17] C. H. Bennett *et al.*, *Phys. Rev. Lett.* **70**, 1895 (1993).
- [18] W. P. Bowen *et al.*, *Phys. Rev. A* **67**, 032302 (2003).
- [19] T. C. Zhang, K. W. Goh, C. W. Chou, P. Lodahl, and H. J. Kimble, *Phys. Rev. A* **67**, 033802 (2003).
- [20] N. Takei, H. Yonezawa, T. Aoki, and A. Furusawa, *Phys. Rev. Lett.* **94**, 220502 (2005).
- [21] N. Takei *et al.*, *Phys. Rev. A* **72**, 042304 (2005).
- [22] X. Jia *et al.*, *Phys. Rev. Lett.* **93**, 250503 (2004).
- [23] S. Lloyd and S. L. Braunstein, *Phys. Rev. Lett.* **82**, 1784 (1999).
- [24] A. Ourjoumtsev, R. Tualle-Brouri, J. Laurat, and P. Grangier, *Science* **312**, 83 (2006).
- [25] J. S. Neergaard-Nielsen, B. M. Nielsen, C. Hettich, K. Mølmer, and E. S. Polzik, *Phys. Rev. Lett.* **97**, 083604 (2006).
- [26] A. Zavatta, S. Viciani, and M. Bellini, *Science* **306**, 660 (2004).
- [27] D. E. Browne, J. Eisert, S. Scheel, and M. B. Plenio, *Phys. Rev. A* **67**, 062320 (2003).
- [28] S. Olivares, M. G. A. Paris, and R. Bonifacio, *Phys. Rev. A* **67**, 032314 (2003).
- [29] H. Nha and H. J. Carmichael, *Phys. Rev. Lett.* **93**, 020401 (2004).
- [30] R. Garcia-Patrón *et al.*, *Phys. Rev. Lett.* **93**, 130409 (2004).
- [31] M. Sasaki and S. Suzuki, *Phys. Rev. A* **73**, 043807 (2006).
- [32] K. Mølmer, *Phys. Rev. A* **73**, 063804 (2006).
- [33] R. W. P. Drever *et al.*, *Appl. Phys. B: Photophys. Laser Chem.* **31**, 97 (1983).
- [34] E. S. Polzik, J. Carri, and H. J. Kimble, *Appl. Phys. B: Photophys. Laser Chem.* **55**, 279 (1992).
- [35] Of course, it would be better if we could use very low frequencies near 0 Hz. In practice, however, very low-frequency components below 5 kHz are often neglected in non-Gaussian-state creation with photon subtraction [25]. In that sense, we can also neglect very low-frequency components for the application of teleportation of such non-Gaussian states.
- [36] K. Yoshino, T. Aoki, and A. Furusawa, quant-ph/0609116.